Research Square

Preprints are preliminary reports that have not undergone peer review.
They should not be considered conclusive, used to inform clinical practice,
or referenced by the media as validated information.

TGFβ1 and BMP9 signal laterally through direct type I receptor cross-activation on a type II receptor scaffold

Michael Trumpp
Freie Universität Berlin
Kjell Bruckmann
Freie Universität Berlin
Sophia Mähr
Freie Universität Berlin
Jerome Jatzlau
Freie Universität Berlin
Petra Knaus
petra.knaus@fu-berlin.de

Freie Universität Berlin

Research Article

Keywords: Lateral signaling, TGFβ receptors, BMP receptors, Receptor cross-activation, Dimerization, SMAD signaling

Posted Date: October 15th, 2026

DOI: https://doi.org/10.21203/rs.3.rs-11077820/v1

License: This work is licensed under a Creative Commons Attribution 4.0 International License.
Read Full License

Additional Declarations: No competing interests reported.

Abstract

Transforming growth factor β (TGFβ) and bone morphogenetic protein (BMP) signaling are conventionally viewed as distinct signaling branches that activate SMAD2/3 and SMAD1/5, respectively. However, TGFβ can also activate SMAD1/5 and BMPs can activate SMAD2/3, a phenomenon termed lateral signaling. Such responses have been proposed to arise through cross-activation between type I receptors of opposing SMAD specificity, but whether full-length receptors can directly cross-activate, whether this extends broadly across receptor pairs, and how type II receptors contribute to lateral signaling remain unresolved. Here we show that type I receptors directly cross-activate one another when brought into close proximity. Chemically induced dimerization revealed that cross-activation can occur in either direction between ALK5 and ALK1, ALK3 or ALK6, and between ALK1 and ALK4. Under ligand stimulation, lateral TGFβ1 and BMP9 signaling required TGFBR2 and ACVR2B, respectively. Their kinase domains catalytically activated the canonical type I receptor while also providing the scaffold required for its subsequent cross-activation of a type I receptor of opposing specificity. Lateral signaling is therefore not a leak between pathways but a defined receptor-level mechanism, in which the type II receptor enables a sequential mechanism of one type I to act on the second type I receptor within the same complex.

Introduction

The transforming growth factor β (TGFβ) and bone morphogenetic protein (BMP) ligands signal through a highly conserved and tightly regulated system essential for development and tissue homeostasis. Both branches often induce opposing biological responses, yet they share a common receptor architecture, activation mechanism and downstream effectors. Already in the absence of ligand, type I (ALK1–ALK7) and type II receptors (TGFBR2, ACVR2A, ACVR2B, BMPR2) associate at the plasma membrane in preformed complexes of varying stability (Nohe et al. 2002; Marom et al. 2011; Ehrlich et al. 2012). Different type I receptors thereby compete for a shared type II receptor(Szilágyi et al. 2022). Ligand binding then assembles two type I and two type II receptors into a tetrameric signaling complex, with type I receptors acting as the high-affinity partners for BMPs and type II receptors for TGFβs (Yadin, Knaus, and Mueller 2016; Jatzlau, Burdzinski, et al. 2023). Within the tetrameric complex, the constitutively active type II kinase phosphorylates the glycine- and serine-rich region (GS box) of a type I receptor and thereby activates its kinase (Huse et al. 2001). The activated type I receptor in turn phosphorylates receptor-regulated SMADs (R-SMADs), which associate with Co-SMAD4 to regulate target gene transcription (Jatzlau et al. 2025). R-SMAD specificity is dictated by the L45 loop of the type I receptor, an eight-residue motif in the kinase domain (Persson et al. 1998). Accordingly, ALK1, ALK2, ALK3 and ALK6 phosphorylate SMAD1/5, whereas ALK4, ALK5 and ALK7 phosphorylate SMAD2/3 (Derynck and Zhang 2003; Katagiri and Watabe 2016).

In canonical TGFβ signaling, the ligand gets bound by its high-affinity receptor TGFBR2, which then activates ALK5, confining the downstream response to SMAD2/3. However, TGFβ3 was also found to induce SMAD1 phosphorylation in breast cancer cells (Liu et al. 1998). Later work showed TGFβ3

activates SMAD1/5 through ALK1 in endothelial cells, an observation dependent on the presence of ALK5 (Goumans et al. 2002; Goumans et al. 2003). The TGFβ-induced ALK1-SMAD1/5 signaling requiring the interaction of and activation by ALK5 was termed lateral signaling. Since ALK1 is largely confined to the endothelium, lateral signaling was initially assumed to be endothelial specific, but it has since been described across a wide range of tissues and cell types (Fig. 1A). In the majority of studies, lateral signaling has been reported for ALK5 activating ALK1 (Valdimarsdottir et al. 2006; Finnson et al. 2008; Blaney Davidson et al. 2009; Nurgazieva et al. 2015; Zhang et al. 2017), or ALK2 or ALK3 in cells lacking ALK1(Bharathy et al. 2008; Daly, Randell, and Hill 2008; Ramachandran et al. 2018). In all cases, the TGFβ high affinity receptor TGFBR2 was required alongside ALK5 (Goumans et al. 2003; Daly, Randell, and Hill 2008). Moreover, loss of the type II receptor BMPR2 enhanced lateral signaling in endothelial cells (Hiepen et al. 2019).

In canonical BMP9 signaling, the ligand is bound by its high-affinity receptor ALK1, which confines the downstream response to SMAD1/5. As for TGFβ, BMP9 was found to activate the opposing SMAD branch, inducing SMAD2 phosphorylation in pulmonary artery endothelial cells (Upton et al. 2009). BMP9-induced activation of SMAD2/3 requiring both ALK1 and ALK5 was subsequently also shown in fibroblasts (Muñoz-Félix et al. 2016). Lateral signaling has further been reported downstream of BMP2 and BMP4, with ALK2, ALK3 or ALK6 acting together with ALK4, ALK5 or ALK7 (Murakami et al. 2009; Holtzhausen et al. 2014; Zhang et al. 2016; Zhao et al. 2018).

Together, these studies establish TGFβ- and BMP-induced lateral signaling across many tissues (Fig. 1A). Receptor knockdown and pharmacological inhibition of selected kinase activities implicated distinct type I receptor pairings, in a cell type- and ligand-specific manner. On a mechanistic level, direct cross-activation has been shown only for the ALK5 and ALK2 kinase domains (Ramachandran et al. 2018). Whether direct activation between type I receptors is restricted to this pair, occurs between full-length receptors, and equally sufficient works in both directions has remained open. We therefore forced defined pairs of Halo- and SNAP-tagged full-length receptors into proximity by chemically induced dimerization (Trumpp et al. 2025). Direct cross-activation by constitutively active type I receptors was observed across all tested type I receptor pairs. Whereas the presence of the type II receptor was reported to be required for lateral signaling, its role beyond activating the canonical type I receptor remained unclear. We found that in both TGFβ1- and BMP9-induced lateral signaling the kinase domain of the respective type II receptor was required for type I receptor cross-activation, not acting catalytically but as a scaffold.

Results

Forced proximity reveals direct, kinase-dependent cross-activation between type I receptors in either direction

TGFβ and BMP induced lateral signaling has been observed across many cell types, tissues, and species(Liu et al. 1998; Goumans et al. 2002; Goumans et al. 2003; Valdimarsdottir et al. 2006; Daly,

Randell, and Hill 2008; Finnson et al. 2008; Upton et al. 2009; Bharathy et al. 2008; Murakami et al. 2009; Blaney Davidson et al. 2009; Holtzhausen et al. 2014; Nurgazieva et al. 2015; Muñoz-Félix et al. 2016; Zhang et al. 2016; Zhang et al. 2017; Ramachandran et al. 2018; Zhao et al. 2018; Hiepen et al. 2019) (Fig. 1A). Yet most of this evidence remains correlative or based on loss-of-function and small molecule inhibitor approaches. Systematic evidence that one type I receptor can activate another directly to elicit the non-canonical R-SMAD response has remained limited. Lateral signaling could originate from clustered type I receptors (Ramachandran et al. 2021) or a mixed tetrameric receptor complex (Ehrlich et al. 2012), in which the canonical type I receptor activates a non-canonical type I receptor, which then signals through its associated R-SMAD (Fig. 1B). To test this directly, we developed a strategy to force defined receptor pairs into proximity and ask whether the canonical receptor can activate the non-canonical receptor and elicit its downstream SMAD response.

For this, we combined constitutively active kinase receptor mutants with a chemically induced dimerization system, using CRISPR/Cas9 knockout HEK293T lines devoid of endogenous TGFβ and BMP type I receptors (**Supp** Fig. 1, 2). First, a constitutively active ALK5 (caALK5) was generated by introducing the T204D mutation into ALK5-Halo (Charng et al. 1998), rendering the receptor active independently of TGFβ1. Bifunctional Halo/SNAP dimerizers of varying linker length (Trumpp et al. 2025) were then used to force caALK5-Halo into proximity with wild-type SNAP-ALK1 (Fig. 1C,D). The dimerizer set comprises BG-PEG_2-HTL, BG-PEG_6-HTL and BG-PEG_{12}-HTL, with linker lengths of approximately 7, 21 and 42 Å. Previously, a conceptually related approach using light-induced dimerization of isolated, membrane-anchored ALK2 kinase and caALK5 kinase domains demonstrated direct activation of ALK2 by ALK5 (Ramachandran et al. 2018). Our chemically induced Halo/SNAP dimerization system extends this principle to full-length receptors. By tethering the receptors only at their N-terminal extracellular tags, the intracellular kinase domains remain free to adopt their native positioning. Successful heterodimerization was confirmed by receptor-dimer bands at approximately 250 kDa in both the Halo and SNAP blots. caALK5 elevated pSMAD2 relative to wild-type ALK5, confirming its constitutive activity, and co-expression of ALK1 raised basal pSMAD1/5 (Fig. 1D). Most importantly, forcing caALK5 and ALK1 together induced lateral pSMAD1/5, with the strongest effect at the shortest linker (BG-PEG_2-HTL).

To test the reciprocal direction, we generated a constitutively active ALK1 (caALK1) carrying the Q201D mutation (Ricard et al. 2010; Kraehling et al. 2016) forced it into proximity with wild-type SNAP-ALK5 (Fig. 1E,F). As before, caALK1 increased pSMAD1/5 independently of stimulation, confirming its activity, and co-expression with ALK5 raised basal pSMAD2. Dimerization of caALK1 and ALK5 further significantly induced lateral pSMAD2 using the PEG_2 linker (Fig. 1F). Forced proximity thus drives direct cross-activation in both directions, with active ALK5 inducing ALK1-dependent pSMAD1/5 and active ALK1 inducing ALK5-dependent pSMAD2.

We next asked how ligand binding and assembly of the tetrameric receptor complex affect type I receptor cross-activation, and which type II receptor most effectively supports this process. We generated kinase-dead mutants of both ALK1 and ALK5 by replacing the catalytic lysine (Goumans et al. 2003; Lux et al. 2005) yielding ALK1-K229R and ALK5-K232R, hereafter refered to as kdALK1 and

kdALK5. Each mutant lost the ability to phosphorylate R-SMADs, confirming loss of kinase activity, as only wild-type ALK5 raised pSMAD2 upon TGFβ1 stimulation and only wild-type ALK1 raised pSMAD1/5 upon BMP9 stimulation (Fig. 2A,D **& Supp** Fig. 3).

Wild-type and kinase-dead ALK5 and ALK1 were co-expressed in all four combinations in ALK2/ALK5 knockout HEK293T cells. TGFBR2 was included to enhance TGFβ1 binding (Baardsnes et al. 2009), and lateral pSMAD1/5 was measured after stimulation (Fig. 2A–C). TGFβ1 significantly induced lateral pSMAD1/5 whenever ALK5 was catalytically active, in presence of both the wild-type ALK1 or the kdALK1. In contrast, replacing ALK5 with kdALK5 abolished the TGFβ1-induced lateral pSMAD1/5. No SMAD1/5 activation was observed when both receptors were kinase-dead. Lateral TGFβ signaling therefore requires the kinase activity of ALK5, the canonical TGFβ type I receptor. Notably, kinase-dead ALK1 did not abolish the lateral SMAD1/5 response entirely, indicating other endogenous type I receptors involved.

We next applied the same kinase-dead strategy to lateral BMP9 signaling. Wild-type and kinase-dead ALK1 and ALK5 were co-expressed in all four combinations together with ACVR2B, which forms BMP9-binding complexes efficiently with ALK1 (Townson et al. 2012), and lateral pSMAD2 was measured (Fig. 2D–F). BMP9 significantly induced lateral pSMAD2 whenever ALK1 was catalytically active, in both the wild-type ALK5 and the kdALK5 combinations. Replacing ALK1 with kdALK1 abolished the stimulation effect, and no BMP9-induced pSMAD2 was detectable in either kdALK1 condition. Lateral BMP9 signaling therefore requires the kinase activity of the canonical type I receptor ALK1. As shown for TGFβ1-induced lateral signaling, inactivating the non-canonical type I receptor, here ALK5, did not abolish the response, indicating that this role may not be restricted to ALK5.

Together, these experiments show that lateral signaling in both directions depends on the kinase activity of the canonical type I receptor, ALK5 for TGFβ1 and ALK1 for BMP9. Interestingly, lateral TGFβ1 signaling persisted when ALK1 was catalytically inactive (Fig. 2A–C), indicating that ALK5 can engage type I receptors other than ALK1. Since ALK2 is absent in these knockout cells, we reasoned that ALK5 might additionally engage the BMP type I receptors ALK3 and ALK6. To test this, we depleted endogenous ALK3 and ALK6 by siRNA in cells expressing wild-type ALK5 or kdALK5 with TGFBR2, and measured lateral pSMAD1/5 after TGFβ1 stimulation (Fig. 3D,G; **Supp** Fig. 4). Expression of ALK5 and TGFBR2 increased basal pSMAD1/5 independent of stimulation to a saturating level, whereas TGFβ1 stimulation further enhanced pSMAD2. Depletion of ALK3 significantly reduced pSMAD1/5 without affecting canonical pSMAD2, and knockdown of ALK6 gave a smaller but significant reduction, in line with its lower endogenous expression (**Supp** Fig. 2). Combined knockdown of ALK3 and ALK6 produced the strongest reduction (**Supp** Fig. 4G–I). In each case the effect was confined to the wild-type ALK5 background; in the kdALK5 background pSMAD1/5 stayed at baseline and was unaffected by ALK3/ALK6 depletion. Transcript knockdown was verified by qPCR (**Supp** Fig. 4).

We then tested whether ALK5 directly cross-activates ALK3 and ALK6 using the dimerization approach. Forcing caALK5 into proximity with ALK3 or ALK6 induced lateral pSMAD1/5, while the reciprocal

pairings of caALK3 or caALK6 with ALK5 induced lateral pSMAD2 (Fig. 3E,F,H,I; **Supp** Fig. 5). The same held true for ALK1 and ALK4, where forced proximity in either direction produced reciprocal lateral signaling (**Supp** Fig. 5), explaining why kinase-dead ALK5 did not abolish BMP9-induced lateral pSMAD2 (Fig. 2D–F). Lateral cross-activation is therefore not confined to the ALK1/ALK5 pair but extends to ALK3/ALK5, ALK6/ALK5, and ALK1/ALK4, indicating that lateral signaling is a general property of TGFβ and BMP type I receptor pairs.

The type II receptor kinase domain scaffolds lateral signaling

As noticed before, co-expression of TGFBR2 enhances both baseline and lateral SMAD1/5 activation (Fig. 2. **& 3**). We next examined if this effect is type II receptor specific. Therefore, we co-expressed ALK1 and ALK5 with β-gal (as control) or with TGFBR2, ACVR2A, ACVR2B, or BMPR2, and measured lateral pSMAD1/5 after TGFβ1 stimulation (Fig. 4A–C). BMP type II receptors raised overall pSMAD1/5 levels (Fig. 4B). Comparing each receptor to its own unstimulated control revealed that only TGFBR2 produced a significant TGFβ1-induced lateral pSMAD1/5 response (Fig. 4C). Lateral TGFβ signaling therefore requires the canonical type II receptor TGFBR2.

We next assessed whether TGFBR2 kinase activity facilitates the cross-activation of ALK1 by ALK5. We co-expressed ALK1 with wild-type TGFBR2, a kinase-dead point mutant (kdTGFBR2, K277R (Wrana et al. 1992; Chung et al. 2019)), or a kinase-domain deletion retaining only the extracellular and transmembrane domains (TGFBR2Δkinase). Because TGFBR2Δkinase can no longer activate ALK5, we used constitutively active ALK5 (caALK5), expressed in A2/A5 KO cells (Fig. 4D–F). Beforehand, we confirmed that TGFBR2Δkinase still localizes to the membrane and binds TGFβ1. Further, kdTGFBR2 was shown to be catalytically inactive in a $CAGA_{12}$-reporter gene assay (**Supp** Fig. 6). Strikingly, in the presence of caALK5 and ALK1 wild-type and kdTGFBR2 enhanced pSMAD1/5 equally independent of ligand, whereas TGFBR2Δkinase showed no increase above control (Fig. 4D–F). The kinase domain of TGFBR2 is thus essential for pSMAD1/5 activation, yet its catalytic activity is dispensable for lateral cross-activation, revealing that the domain acts as a structural scaffold rather than as a catalyst.

To confirm this scaffold role, we tested whether the ALK1–ALK5 interaction is preserved when the TGFBR2 kinase domain is deleted. We co-immunoprecipitated myc-ALK1 with ALK5 in the presence of wild-type TGFBR2 or TGFBR2Δkinase (Fig. 4G). ALK1 associated equally with ALK5, TGFBR2, and TGFBR2Δkinase, independently of the kinase domain and of TGFβ1 stimulation. Accordingly, the TGFBR2 kinase domain is required for lateral signaling but not for the interaction between the receptors, consistent with a scaffolding signaling role. The interaction persisted even when the ALK1 extracellular domain was removed, indicating that transmembrane contacts are sufficient for the interaction (**Supp Fig. 7**).

We next asked which type II receptor supports lateral BMP9 signaling. ALK1 and ALK5 were co-expressed with β-gal or with TGFBR2, ACVR2A, ACVR2B, or BMPR2, and lateral pSMAD2 was measured after BMP9 stimulation (Fig. 5A–C). Overall pSMAD2 levels varied considerably and with a high baseline

across different type II receptors (Fig. 5B). Comparing each receptor to its own unstimulated control revealed that only ACVR2B produced a significant BMP9-induced increase in lateral pSMAD2 (Fig. 5C). This is independent of the type II receptors capability to interact with ALK1 and ALK5 (**Supp Fig. 8A,B**). ALK1 and ALK5 co-immunoprecipitated TGFBR2, ACVR2A, and ACVR2B at a comparable level independent of BMP9, but co-immunoprecipitated BMPR2 only weakly.

To further test if the BMP9-induced lateral signaling is also dependant on a scaffolding role of the type II receptor kinase, we tested for lateral pSMAD2 in the presence of kinase-dead variants of each type II receptor (kdTGFBR2, kdACVR2A, kdACVR2B, and kdBMPR2 (Bagarova et al. 2013)), each confirmed catalytically inactive (**Supp Fig. 8C**). Since a kinase-dead type II receptor can no longer activate ALK1, we used caALK1, co-expressed with ALK5 (Fig. 5D–F). Among the four receptors, only kdACVR2B supported a significant BMP9-induced increase in lateral pSMAD2 above the β-gal control. ACVR2B thus supports lateral BMP9 signaling even without its kinase activity, pointing to a non-catalytic role. In contrast, in presence of kdBMPR2 BMP9-induced lateral pSMAD2-induction was abolished. This is line with previous reports that described BMPR2 as gatekeeper of aberant TGFβ signaling, including elevated TGFβ1-induced lateral signaling in absence of BMPR2 (Hiepen et al. 2019).

As BMPR2 can be distinguished from other type II receptors by its unique long C-terminal cytoplasmic tail, we next asked whether depletion of the C-terminus would enhance lateral signaling. However, BMPR2-Short Form (SF), a tail-truncated variant (**Supp Fig. 9A**), still failed to enhance lateral pSMAD2, similarly to full-length BMPR2 (**Supp Fig. 9B**), despite an increased interaction with ALK1 and ALK5 (**Supp Fig. 9C**).

The non-catalytic contribution of ACVR2B suggested that its kinase domain similar to TGFBR2 acts as a scaffold for lateral type I kinase cross-activation. To test this, we generated a kinase-domain deletion mutant (ACVR2BΔkinase) that is still able to localize to the membrane and bind its high affinity ligand (**Supp Fig. 10**). We then compared wild-type ACVR2B, kinase-dead ACVR2B, and ACVR2BΔkinase for their ability to support ALK1 activation of ALK5, using again caALK1 to bypass the type II receptor's role in activating ALK1 (Fig. 6A–C). Interestingly, both wild-type and kinase-dead ACVR2B enhanced significantly BMP9-induced lateral pSMAD2, whereas ACVR2BΔkinase failed to enhance it (Fig. 6A–C). Once ALK1 is active, ACVR2B no longer requires its catalytic activity to support lateral signaling, yet its kinase domain remains essential, indicating that the domain acts as a structural scaffold for lateral cross-activation of type I receptors. To further confirm this scaffold role, we tested whether ALK1/5 interaction with ACVR2B is preserved when the ACVR2B kinase domain is deleted. Co-immunoprecipitation of myc-ALK1 or myc-ALK5 showed that both interacted equally with ACVR2B and ACVR2BΔkinase, and the ALK1-ALK5 interaction itself was unaffected by the deletion (Fig. 6D). The ACVR2B kinase domain is therefore required for lateral signaling but not for the interaction between the receptors, as found for TGFBR2 (Fig. 4).

Finally, we investigated why ACVR2B, but not ACVR2A, supports lateral BMP9 signaling (Fig. 5), given that both interact comparably with ALK1 and ALK5 (**Supp. Figure 8**). Therefore, we swapped the

extracellular domains (ECD) of both receptors. We generated kinase-dead ACVR2A/B ECD chimeras to exclude catalytic activity (**Supp Fig. 11A**). Only receptors carrying the ACVR2B extracellular domain supported BMP9-induced lateral pSMAD2, whereas those carrying the ACVR2A extracellular domain did not (**Supp Fig. 11B**). The difference between ACVR2A and ACVR2B in lateral signaling therefore resides in the extracellular domain, not the kinase domain. This is in line with the higher BMP9 affinity of ACVR2B relative to the other type II receptors (Townson et al. 2012). The ACVR2B extracellular domain thus provides efficient BMP9 binding, potentially promoting assembly of the signaling complex, while its kinase domain scaffolds lateral activation.

Discussion

We previously used chemically induced dimerization to bring TGFβ and BMP receptors into proximity and found that pairing a type I with a type II receptor, ALK1 with ACVR2B or ALK5 with TGFBR2, did not elicit a SMAD response (Trumpp et al. 2025). Here, forcing two type I receptors together induced lateral signaling when one of them was constitutively active, while two wild-type type I receptors gave no response. This indicates that activating a type I receptor through a type II receptor requires more than proximity. Within a type I / type II kinase heterodimer, the GS domain, the transactivation domain within the type I receptor, faces away from the type II active site and cannot be phosphorylated, so activation requires a second heterodimer to associate and present the GS domains to the type II kinases (Agnew et al. 2021). In contrast, a constitutively active type I receptor is already in the active state and can therefore act on a wild-type type I partner within a single pair, without the need for tetramer assembly. In addition to the requirement of an active type I receptor, cross-activation was sensitive to the dimerizer length. The shortest dimerizer (BG-PEG_2-HTL) always gave the strongest lateral activation, although the difference from the intermediate dimerizer (BG-PEG_6-HTL) was not significant in every pair. This points to cross-activation between type I receptors being favored by a more constrained arrangement rather than by proximity alone, since a shorter tether reduces the range of relative positions accessible to the two receptors and their kinases.

Lateral signaling did not depend exclusively on ALK1 in the TGFβ context or on ALK5 in the BMP9 context. Inactivation of the respective receptor kinase did not abolish the response, suggesting that other type I receptors can substitute as signaling partners. Consistent with this, mixed type I receptor complexes have previously been proposed, involving ALK1 or ALK2 alongside ALK5 in TGFβ signaling (Goumans et al. 2003; Finnson et al. 2008; Daly, Randell, and Hill 2008; Ramachandran et al. 2018) and ALK1, ALK3 or ALK6 alongside ALK4/ALK5 in BMP signaling (Murakami et al. 2009; Holtzhausen et al. 2014; Zhao et al. 2018). These studies provided important evidence that mixed type I receptor complexes contribute to lateral signaling. The approaches used, however, could not determine whether full length type I receptor directly activates another within these complexes. Our findings extend this work by showing that the reported signaling relationships are mediated by direct type I receptor cross-activation. TGFβ has also been reported to induce SMAD1/5 through ALK5 alone(Liu et al. 2009; Wrighton et al. 2009; van Caam et al. 2017). Such a contribution may add to the background pSMAD

levels in our system, but it would not explain a cross-activation or the linker-length dependence we observe. Among the receptors tested, lateral activation was therefore not restricted to specific receptor pairs but appears to be a broader property of the type I receptor family. Which receptor combinations are engaged *in vivo* is likely determined by their relative expression levels in a given cellular context (Murakami et al. 2009).

Further, the type II receptor is needed for lateral signaling within the native tetrameric receptor complex, though not only for the reason expected. Its kinase domain is required for cross-activation between the type I receptors, beyond its role in activating the canonical type I receptor. Deleting the type II kinase domain abolished lateral signaling, yet the type I and II receptors still interacted. Further the kinase dead domain supported lateral signaling as well as the wild type. The type II kinase domain is therefore required not as an enzyme but as a scaffold that may position the type I receptor kinases for cross-activation within the tetramer. Efficient TGFβ-induced ALK1 activation was likewise shown to require the intracellular domains of both ALK5 and TGFBR2 (Goumans et al. 2003), and our kinase-dead comparison now resolves the TGFBR2 contribution through a structural rather than catalytic role.

Both type I/type II and type I/type I receptor interactions were detectable in the absence of ligand, consistent with previously described preformed receptor complexes (Gilboa et al. 2000; Nohe et al. 2002; Goumans et al. 2003; Marom et al. 2011). Ligand binding may therefore reorganize or stabilize pre-existing receptor assemblies, either by bringing two preformed type I/type II dimers together or by recruiting type II receptors to a preformed type I receptor pair. Under either model, lateral signaling would be determined during complex assembly by the identity of the type I receptor incorporated alongside the canonical signaling receptor. This predicts an asymmetry between lateral TGFβ and BMP9 signaling because ligand affinity is distributed differently across their receptor complexes. In TGFβ receptor complexes, the type II receptor binds the ligand with higher affinity than the type I receptor, whereas in BMP receptor complexes, the type I receptor generally provides the higher-affinity interaction (Heldin and Moustakas 2016). Accordingly, TGFβ capture depends primarily on TGFBR2, making the identity of the incorporated type I receptor comparatively less restrictive. By contrast, ALK1 is itself the high-affinity BMP9 receptor (Kienast et al. 2016; Jatzlau, Burdzinski, et al. 2023), which may favor complexes in which both type I receptor positions on the ligand (wrist epitopes, (Townson et al. 2012)) are occupied by ALK1. Incorporating a non-canonical type I receptor should therefore be less constrained in TGFβ complexes than in BMP9 complexes.

The same logic may explain which type II receptor supports lateral BMP9 signaling. Although ACVR2A and ACVR2B interacted comparably with the type I receptors, only ACVR2B supported the lateral response. Domain-swapping experiments further showed that replacing the ACVR2A extracellular domain with that of ACVR2B enabled the ACVR2A kinase domain to support lateral signaling, revealing its capacity to organize the receptor complex once efficient ligand capture was provided. The contribution of the type II receptor can therefore be separated into (1) ligand capture by the extracellular domain and (2) receptor-complex organization by the intracellular kinase domain, consistent with the higher affinity of ACVR2B for BMP9 among the type II receptors (Townson et al. 2012). By contrast,

BMPR2 did not support lateral signaling in neither the TGFβ- nor BMP9-induced setting. Similarly, knockdown of ACVR2A or ACVR2B, but not BMPR2, has been shown to reduce BMP9-induced SMAD1/5 signaling (Szilágyi, Gutman, and Henis 2022). Conversely, loss of BMPR2 in endothelial cells enhanced lateral responses, an effect attributed to BMPR2 restricting the formation of mixed receptor complexes (Hiepen et al. 2019). The extent of lateral signaling may therefore also be shaped by the type II receptor expression profile of a given cell.

Lateral signaling has been associated with distinct cellular outcomes in settings ranging from vasculogenesis to cancer, where it accompanies the canonical response (Goumans et al. 2002; Holtzhausen et al. 2014). In mammary epithelial cells TGFβ-induced SMAD3 activity is required together with a transient TGFβ-induced pSMAD1/5 for the onset of epithelial to mesenchymal transition (Ramachandran et al. 2018). Both the amount and the composition of the SMAD complexes formed would determine the transcriptional targets. First, how much lateral-induced R-SMAD is generated should depend on how many lateral complexes form, and therefore on the receptors and ligands available to the cell. Consequently, the amount of lateral-induced R-SMAD would determine the target genes selection, as some target genes are activated at low doses of pSMAD and others require higher doses (Jatzlau, Mendez, et al. 2023). ID genes represent a class of low dose SMAD target genes (Jatzlau, Mendez, et al. 2023), and were reported to be induced by TGFβ-induced pSMAD1/5 (Ramachandran et al. 2018). Second, complexes in which the canonical and the non-canonical type I receptor are both active, generate the two R-SMAD species at the same complex. This could favor the formation of mixed SMAD complexes. These have indeed been detected where lateral signaling is enhanced (Daly, Randell, and Hill 2008; Hiepen et al. 2019), and would read regulatory elements by rules differing from those of either canonical complex (Itoh et al. 2019; Jatzlau et al. 2025). Lateral signaling may therefore produce a mixed transcriptional output, combining both branches within the same response.

Together, previous work and our findings support a stepwise model for lateral signaling. Established models suggest that (1) ligand capture is determined primarily by the receptor subunit with the highest ligand affinity and (2) ligand binding promotes assembly of a heterotetrameric complex from preformed type I/type I or type I/type II receptor dimers. Our data directly supports that (3) the type II receptor activates the canonical type I receptor within the mixed type I receptor complex. We further show that (4) the activated canonical type I receptor directly cross-activates an adjacent type I receptor of opposing R-SMAD specificity, while the type II receptor kinase domain serves as a scaffold in this process. This mechanism raises the possibility that (5) both type I receptors activate their respective R-SMADs originating from the same complex, potentially promoting mixed SMAD complexes and a transcriptional response distinct from that generated by either canonical pathway alone.

Material and Methods

Cell culture and transient transfection

COS-7 and HEK293T cells were obtained from the German Collection of Microorganisms and Cell Cultures (DSMZ). Cells were cultured in Dulbecco's Modified Eagle's Medium (DMEM) supplemented with 10% FCS, 2 mM L-glutamine, and penicillin (100 units/mL)/streptomycin (100 µg/mL) (full medium) in a humidified atmosphere at 37°C and 5% CO_2 (v/v). Cells were maintained sub-confluent and split 1:5 to 1:10 as required. For passaging, cells were washed once with PBS and detached with trypsin/EDTA (0.05/0.02% in PBS). COS-7 and HEK293T cells and their knockout derivatives were transfected 24 h after seeding in 96-well plates, 12-well plates, or 10 cm dishes, using Lipofectamine 2000 (Thermo Fisher Scientific), Lipofectamine 3000 (Thermo Fisher Scientific), or PEI (Sigma-Aldrich) according to the manufacturer's instructions and the experimental setting. Transfection mixes were added directly to the medium without a prior wash step.

CRISPR/CAS9-mediated genome editing

ALK5 knockout HEK293T lines were generated by targeting two distinct sites in exon 2 of the *TGFBR1* gene with separate sgRNAs. Target sites were identified using CHOPCHOP (Labun et al. 2019). The guide sequences were named G2 (5'-CATACAAACGGCCTATCTCGAGG-3') and G12 (5'-TGGCAGAAACACTGTAACGCTGG-3') according to their CHOPCHOP rank. HEK293T cells were seeded in 6-well plates at 500,000 cells per well in 3 mL DMEM growth medium. After 24 h, cells were transfected with 2 µg per well of the pX458 plasmid, encoding Cas9, eGFP, and the respective sgRNA, using Lipofectamine 2000. After 48 h, cells were detached by trypsinization, resuspended in fluorescence-activated cell sorting (FACS) buffer, and sorted for eGFP-positive cells, with single eGFP-positive cells deposited into individual wells of a 96-well plate. Clones were cultured in high-glucose DMEM (4.5 g/L glucose, 20% FCS) to promote proliferation, and surviving clones were expanded stepwise into 24-well and then 12-well plates according to confluency. Each clone was split into two cultures: one expanded for cryopreservation and one used for genomic DNA isolation and knockout validation by Sanger sequencing.

Molecular cloning

Cloning and genotyping PCRs were performed on a Peltier Thermal Cycler PTC-200 using Phusion polymerase, with elongation times adjusted to product size (~ 1 kb/min). All primers used for PCR are listed in (**Supp. Table 1**) PCR products were resolved by agarose gel electrophoresis and purified using the NucleoSpin Gel and PCR Clean-up kit (Macherey-Nagel). Unless stated otherwise, ligation or assembly products were transformed into chemically competent DH5α *E. coli* by heat shock and plated on LB-agar containing Ampicillin or Kanamycin. Plasmid DNA was purified using the NucleoSpin Plasmid EasyPure kit (Macherey-Nagel), and constructs were verified by Sanger and whole-plasmid sequencing.

Cloning of the sgRNA constructs. Complementary oligonucleotides carrying the sgRNA sequence and a 5' BbsI overhang were phosphorylated and annealed with T4 polynucleotide kinase. The pX458 plasmid was linearized with BbsI, and the annealed oligonucleotides were ligated into it with T4 DNA ligase. sgRNA integration was confirmed by Sanger sequencing.

gDNA extraction and TOPO cloning. To verify CRISPR/Cas9-induced mutations in exon 2 of the *TGFBR1* gene, genomic DNA was extracted from single HEK293T clones using QuickExtract DNA Extraction Solution 1.0 (Biosearch Technologies). The region spanning the targeted sites was amplified by PCR, and the purified product was blunt-end ligated into the pCR-Blunt II-TOPO vector using the Zero Blunt TOPO PCR Cloning kit (Thermo Fisher Scientific). Following transformation into DH5α *E. coli*, five clones per sample were Sanger-sequenced to confirm the presence and nature of the introduced mutations.

Gibson cloning of Halo- and SNAP-tagged BMP receptor mutants. Halo- and SNAP-tagged BMP receptor mutants were generated from existing pcDNA3.1 BMP receptor constructs by Gibson assembly. Overlapping oligonucleotides carrying the desired mutation were designed within the receptor ORF, together with a second overlapping primer pair in the backbone, yielding two PCR fragments per plasmid for reassembly. Fragments were joined using the NEBuilder HiFi DNA Assembly kit (New England Biolabs) and transformed into the supplied NEB 5-alpha competent *E. coli*.

Ligand- and dimerizer-induced signaling assays

HEK293T cells were seeded in 12-well plates at 150,000 cells per well and transfected 24 h later using Lipofectamine 2000 (ligand stimulation) or Lipofectamine 3000 (dimerization experiments). Cells were transfected with a total of 500 ng plasmid DNA per well, with the amount of each construct adjusted to achieve comparable receptor expression. In control conditions, β-galactosidase (β-gal) plasmid was transfected in place of the omitted receptor to maintain equal DNA amounts. The following day, cells were starved in serum-free DMEM for 3 h and then stimulated by adding ligand or dimerizer to the medium: 0.2 nM TGFβ1 for 30 min, 0.3 nM BMP9 for 60 min, or 0.5 µM of the indicated dimerizer for 30 min. Cells were lysed in 1x Laemmli buffer and analyzed by immunoblotting.

Bifunctional dimerizer molecules consist of a benzylguanine (BG) group and a HaloTag ligand (HTL) joined by a polyethylene glycol (PEG) linker. The BG group reacts covalently with the SNAP-tag and the HTL with the HaloTag, bridging receptors carrying the respective tags. Three variants were used, BG-PEG_2-HTL, BG-PEG_6-HTL and BG-PEG_{12}-HTL, with linker lengths of approximately 7, 21 and 42 Å. Synthesis and characterization are described in (Trumpp et al. 2025).

SDS-PAGE and immunoblotting

Cell lysates were thawed, homogenized by passage through a syringe, boiled at 95°C for 15 min, and resolved on 10% polyacrylamide gels by SDS-PAGE. Proteins were transferred to PVDF membranes, blocked for 1 h (3% BSA), and incubated overnight at 4°C with primary antibodies against GAPDH (Cell Signaling, #2118; 1:5000), Halo (Promega, #G9211), SNAP (Invitrogen, #CAB4255), pSMAD1/5 (Cell Signaling, #9516), pSMAD2 (Cell Signaling, #3108S), and myc (in-house), each at 1:1000 unless stated otherwise. Membranes were washed three times for 5 min in TBS-T, incubated for 1 h with HRP-conjugated goat anti-mouse or anti-rabbit secondary antibodies (Dianova, #115-035-068, #111-035-144;

1:10,000), and washed again three times for 5 min in TBS-T. Signals were developed with WesternBright Quantum HRP substrate (Advansta) and imaged on a FUSION FX7 system.

Dual-luciferase reporter assay

HEK293T cells were seeded in 96-well plates at 50,000 cells per well and transfected 24 h later with PEI. Each well received 50 ng of each receptor construct, 50 ng of the firefly reporter (BRE-luciferase reporter for pSMAD1/5/8 or $CAGA_{12}$-luciferase reporter for pSMAD2/3), and 30 ng of the *Renilla* luciferase control reporter (RLTK). Twenty-four hours after transfection, cells were starved in serum-free DMEM for at least 3 h and, where indicated, stimulated with ligand for a further 24 h. Cells were lysed in 1x Passive Lysis Buffer, and luciferase activity was measured on a Tecan Spark microplate reader. Firefly luminescence was normalized to *Renilla* luminescence unless otherwise stated.

Quantitative real-time PCR (qPCR)

Total RNA was isolated using the NucleoSpin RNA kit (Macherey-Nagel) according to the manufacturer's instructions. cDNA was synthesized from 1000 ng RNA using M-MuLV Reverse Transcriptase and the corresponding reaction buffer (New England Biolabs) with random primers. Quantitative PCR was performed with the Luna Universal qPCR Master Mix (New England Biolabs) on an Applied Biosystems StepOnePlus system (Thermo Fisher Scientific), using 2.5 ng cDNA per reaction in a 10 µL total volume. Target genes were quantified relative to the housekeeping gene *RPS9* using the ΔΔCt method, and measurements were performed as three technical replicates. All primers used for qPCR are listed in (**Supp. Table 2**)

Co-immunoprecipitation

COS-7 cells were seeded in 10 cm dishes (1,000,000 cells per dish) and transfected the next day with PEI (2500 ng per construct). In each experiment, a myc-tagged receptor was co-expressed with Halo-tagged candidate interaction partners. Twenty-four hours after transfection, cells were starved for 24 h and then either harvested directly or stimulated for 30 min with 0.2 nM TGFβ1 or 0.3 nM BMP9 to assess the effect of ligand on complex formation. Cells were then washed with cold PBS and lysed in RIPA buffer for 45 min at 4°C, and lysates were cleared by centrifugation. An aliquot of each cleared lysate was retained as total cell lysate (TCL) input, and the remaining supernatant was split equally and incubated overnight at 4°C with either a mouse anti-myc antibody or normal mouse IgG (IgG control). The antibody-bound complexes were precipitated with rProtein A Sepharose Fast Flow beads (Cytiva) for 90 min at 4°C, washed three times with cold RIPA buffer, and eluted in 2x Laemmli buffer. Samples were treated with DTT prior to SDS-PAGE to reduce and separate antibody heavy and light chains. To avoid detection of the mouse IgG heavy chain, which overlaps with target proteins, a goat anti-mouse IgG light-chain-specific HRP-conjugated secondary antibody was used for immunoblotting.

siRNA knockdown of endogenous receptors

For knockdown of endogenous type I BMP receptors, HEK293T cells were seeded in 12-well plates (150,000 cells per well) and transfected the next day with target siRNA or non-targeting control siRNA

(scrRNA) at 40 nM using Lipofectamine 2000. ALK3 (*BMPR1A*) was targeted with siRNA A-004933-20-0020, ALK6 (*BMPR1B*) with a pool of siRNAs A-004934-14-0005 and A-004934-15-0005, and the non-targeting control was D-001910-01-50 (all Dharmacon). The following day, cells were transfected a second time with the receptor constructs (500 ng per well) using Lipofectamine 2000 and incubated for a further 48 h. Cells were then starved, stimulated, and harvested as described for the signaling assays.

Ligand surface binding assay (LSBA)

To assess whether receptor mutants were expressed and correctly localized, ligand surface binding assays were performed, visualizing both plasma membrane localization and binding of a fluorescently labeled ligand. COS-7 cells were seeded on glass coverslips in 12-well plates (150,000 cells per well) and transfected the next day with 500 ng total plasmid DNA using Lipofectamine 2000. The following day, cells were starved in serum-free DMEM for 3 h and washed with cold PBS. Surface receptors were then labeled with the membrane-impermeable HaloTag ligand HTL-Alexa488 (Promega, #G1002) and the fluorescently labeled ligand for 30 min at 4°C to prevent internalization. Fluorescent ligands were labeled as described (Jatzlau, Burdzinski, et al. 2023). Cells were then washed with cold PBS, fixed in ice-cold methanol for 5 min, and mounted in Fluoromount G. Confocal images were acquired on an Abberior Expert Line STED microscope using 485 nm and 640 nm excitation and processed in Fiji/ImageJ.

Statistical analysis and data presentation

Statistical analyses were performed in GraphPad Prism 9.3, with the specific test for each experiment indicated in the corresponding figure legend. Depending on the experimental design, one- or two-way ANOVA was applied, followed by Tukey's or Dunnett's multiple comparisons test, assuming normal distribution. Statistical significance was defined as $p < 0.05$. Figures were assembled in Adobe Photoshop (Adobe Systems, San José, USA), and schematic illustrations were created with BioRender.

Declarations

Conflict of Interest

The authors declare no competing interest.

Author Contribution

M.T., K.B. and J.J. designed the study, analyzed the data and generated all figures. S.M. performed and analyzed the qPCR experiments. M.T. and K.B. performed all the other experiments, cloned all Halo-receptor constructs and generated the CRISPR ALK5 KO cell lines. M.T., J.J. and P.K. wrote the manuscript. All authors commented on the manuscript.

Acknowledgement

J.J. and P.K. acknowledge the support from Deutsche Forschungsgemeinschaft DFG (SFB1444) and the Einstein Center for Regenerative Therapies (ECRT). M.T. was supported by the Max Planck Research School IMPRS-BAC. Further, the authors would like to thank Wiktor Burdzinski (Freie Universität Berlin) for providing us ALK2 KO and ALK2/ALK4 KO HEK293T cell lines. The authors would like to thank BioRender for providing a platform to generate elements of Figure 1 – 6, Supplemental Figure 1 – 5, Supplemental Figure 1, 7, 9 and 11 (Created in BioRender. Trumpp, M. (2026) https://BioRender.com/dkvma5w).

References

1. Agnew C, Ayaz P, Kashima R, Loving HS, Ghatpande P, Kung JE, Underbakke ES, Shan Y, Shaw DE. Akiko Hata, and Natalia Jura. 2021. 'Structural basis for ALK2/BMPR2 receptor complex signaling through kinase domain oligomerization'. Nat Commun, 12: 4950.
2. Baardsnes J, Hinck CS, Hinck AP, O'Connor-McCourt MD. TbetaR-II discriminates the high- and low-affinity TGF-beta isoforms via two hydrogen-bonded ion pairs. Biochemistry. 2009;48:2146–55.
3. Bagarova J, Vonner AJ, Armstrong KA, Börgermann J, Lai CS, Deng DY, Beppu H, Alfano I, Filippakopoulos P, Morrell NW, Bullock AN, Knaus P, Mishina Y. and P. B. Yu. 2013. 'Constitutively active ALK2 receptor mutants require type II receptor cooperation'. Mol Cell Biol, 33: 2413–24.
4. Bharathy S, Xie W, Yingling JM, Reiss M. Cancer-associated transforming growth factor beta type II receptor gene mutant causes activation of bone morphogenic protein-Smads and invasive phenotype. Cancer Res. 2008;68:1656–66.
5. Blaney Davidson, Esmeralda N, Dennis FG, Remst EL, Vitters, Henk M, van Beuningen AB, Blom M-J, Goumans, Wim B, van den Berg, Peter M, van der Kraan. Increase in ALK1/ALK5 Ratio as a Cause for Elevated MMP-13 Expression in Osteoarthritis in Humans and Mice. J Immunol. 2009;182:7937–45.
6. Charng M-J, Frenkel PA, Lin Q, Yumada M, Schwartz RJ, Olson EN, Overbeek P, Schneider MD. A Constitutive Mutation ofALK5Disrupts Cardiac Looping and Morphogenesis in Mice. Dev Biol. 1998;199:72–9.
7. Chung AK, OuYang CN, Liu H, Chao M, Luo JD, Lee CY, Lu YJ, Chung IC, Chen LC, Wu SM, Tsang NM, Chang KP, Hsu CL, Li HP, Chang YS. Targeted sequencing of cancer-related genes in nasopharyngeal carcinoma identifies mutations in the TGF-β pathway. Cancer Med. 2019;8:5116–27.
8. Daly A, C RA, Randell, and C. S Hill. Transforming growth factor beta-induced Smad1/5 phosphorylation in epithelial cells is mediated by novel receptor complexes and is essential for anchorage-independent growth. Mol Cell Biol. 2008;28:6889–902.
9. Derynck R, Zhang YE. Smad-dependent and Smad-independent pathways in TGF-beta family signalling. Nature. 2003;425:577–84.
10. Ehrlich M, Gutman O, Knaus P, Henis YI. Oligomeric interactions of TGF-β and BMP receptors. FEBS Lett. 2012;586:1885–96.
11. Finnson KW, Wendy L, Parker. Peter ten Dijke, Midory Thorikay, and Anie Philip. 2008. 'ALK1 Opposes ALK5/Smad3 Signaling and Expression of Extracellular Matrix Components in Human

Chondrocytes'. J Bone Miner Res, 23: 896–906.

12. Gilboa L, Nohe A, Geissendörfer T, Sebald W, Henis YI, Knaus P. Bone morphogenetic protein receptor complexes on the surface of live cells: a new oligomerization mode for serine/threonine kinase receptors. Mol Biol Cell. 2000;11:1023–35.
13. Goumans MJ, Valdimarsdottir G, Itoh S, Rosendahl A, Sideras P. and P. ten Dijke. 2002. 'Balancing the activation state of the endothelium via two distinct TGF-beta type I receptors'. Embo j, 21: 1743–53.
14. Goumans M-J, Valdimarsdottir G, Itoh S, Lebrin F, Larsson J, Mummery C, Karlsson S, Peter ten Dijke. Activin Receptor-like Kinase (ALK)1 Is an Antagonistic Mediator of Lateral TGFβ/ALK5 Signaling. Mol Cell. 2003;12:817–28.
15. Heldin CH, Moustakas A. 2016. 'Signaling Receptors for TGF-β Family Members'. Cold Spring Harb Perspect Biol, 8.
16. Hiepen C, Jatzlau J, Hildebrandt S, Kampfrath B, Goktas M, Murgai A. Jose Luis Cuellar Camacho, Rainer Haag, Clemens Ruppert, Gerhard Sengle, Elisabetta Ada Cavalcanti-Adam, Kerstin G. Blank, and Petra Knaus. 2019. 'BMPR2 acts as a gatekeeper to protect endothelial cells from increased TGFβ responses and altered cell mechanics', *PLOS Biology*, 17: e3000557.
17. Holtzhausen A, Golzio C, How T, Lee YH, Schiemann WP, Katsanis N, Blobe GC. Novel bone morphogenetic protein signaling through Smad2 and Smad3 to regulate cancer progression and development. Faseb j. 2014;28:1248–67.
18. Huse M, Muir TW, Xu L, Chen YG, Kuriyan J, Massagué J. The TGF beta receptor activation process: an inhibitor- to substrate-binding switch. Mol Cell. 2001;8:671–82.
19. Itoh Y, Koinuma D, Omata C, Ogami T, Motizuki M, Yaguchi SI, Itoh T, Miyake K, Tsutsumi S, Aburatani H, Saitoh M, Miyazono K, Miyazawa K. A comparative analysis of Smad-responsive motifs identifies multiple regulatory inputs for TGF-β transcriptional activation. J Biol Chem. 2019;294:15466–79.
20. Jatzlau J, Do SN, Mees RA, Mendez PL, Khan RJ, Maas L, Ruiz L, Martin-Malpartida P, Macias MJ, Knaus P. Rare but specific: 5-bp composite motifs define SMAD binding in BMP signaling. BMC Biol. 2025;23:79.
21. Jatzlau J, Burdzinski W, Trumpp M, Obendorf L, Roßmann K, Ravn K, Hyvönen M, Bottanelli F, Broichhagen J, Petra Knaus. A versatile Halo- and SNAP-tagged BMP/TGFβ receptor library for quantification of cell surface ligand binding. Commun Biology. 2023;6:34.
22. Jatzlau J, Mendez P-L, Altay A, Raaz L, Zhang Y, Mähr S, Sesver A, Reichenbach M, Mundlos S, Vingron M, and Petra Knaus. 2023. 'Fluid shear stress-modulated chromatin accessibility reveals the mechano-dependency of endothelial SMAD1/5-mediated gene transcription', *iScience*, 26.
23. Katagiri T, Watabe T. 2016. 'Bone Morphogenetic Proteins'. Cold Spring Harb Perspect Biol, 8.
24. Kienast Y, Jucknischke U, Scheiblich S, Thier M, de Wouters M, Haas A, Lehmann C, Brand V, Bernicke D, Honold K, Stefan Lorenz. Rapid Activation of Bone Morphogenic Protein 9 by Receptor-mediated Displacement of Pro-domains*. J Biol Chem. 2016;291:3395–410.

25. Kraehling JR, Chidlow JH, Rajagopal C, Sugiyama MG, Fowler JW, Monica Y, Lee X, Zhang CM, Ramírez EJ, Park B, Tao K, Chen W, Zhou MW, Nagle WL, Lee. Carlos Fernández-Hernando, and William C. Sessa. 2016. 'Genome-wide RNAi screen reveals ALK1 mediates LDL uptake and transcytosis in endothelial cells', *Nature Communications*, 7: 13516.
26. Labun K, Montague TG, Krause M, Yamila N, Torres Cleuren. Håkon Tjeldnes, and Eivind Valen. 2019. 'CHOPCHOP v3: expanding the CRISPR web toolbox beyond genome editing'. Nucleic Acids Res, 47: W171–74.
27. Liu IM, Schilling SH, Knouse KA, Choy L, Derynck R, Xiao-Fan W. TGFβ-stimulated Smad1/5 phosphorylation requires the ALK5 L45 loop and mediates the pro-migratory TGFβ switch. EMBO J. 2009;28:88–98.
28. Liu X, Yue J, Frey RS, Zhu Q, Mulder KM. Transforming growth factor beta signaling through Smad1 in human breast cancer cells. Cancer Res. 1998;58:4752–7.
29. Lux A, Beil C, Majety M, Barron S, Gallione CJ, Kuhn H-M, Berg JN, Kioschis P, Marchuk DA, and Mathias Hafner. Human Retroviral gag- and gag-pol-like Proteins Interact with the Transforming Growth Factor-β Receptor Activin Receptor-like Kinase 1*[boxs]. J Biol Chem. 2005;280:8482–93.
30. Marom B, Heining E, Knaus P, Henis YI. Formation of stable homomeric and transient heteromeric bone morphogenetic protein (BMP) receptor complexes regulates Smad protein signaling. J Biol Chem. 2011;286:19287–96.
31. Muñoz-Félix JoséM, Cuesta C, Perretta-Tejedor N, Subileau M, Francisco J, López-Hernández JoséM. Identification of bone morphogenetic protein 9 (BMP9) as a novel profibrotic factor in vitro. Cell Signal. 2016;28:1252–61. López-Novoa, and Carlos Martínez-Salgado.
32. Murakami M, Kawachi H, Ogawa K, Nishino Y, Funaba M. Receptor expression modulates the specificity of transforming growth factor-beta signaling pathways. Genes Cells. 2009;14:469–82.
33. Nohe A, Hassel S, Ehrlich M, Neubauer F, Sebald W, Henis YI, Knaus P. The mode of bone morphogenetic protein (BMP) receptor oligomerization determines different BMP-2 signaling pathways. J Biol Chem. 2002;277:5330–8.
34. Nurgazieva D, Mickley A, Moganti K, Ming W, Ovsyi I, Popova A, Sachindra K, Awad N, Wang K, Bieback. Sergij Goerdt, Julia Kzhyshkowska, and Alexei Gratchev. 2015. 'TGF-β1, but Not Bone Morphogenetic Proteins, Activates Smad1/5 Pathway in Primary Human Macrophages and Induces Expression of Proatherogenic Genes'. J Immunol, 194: 709–18.
35. Persson U, Izumi H, Souchelnytskyi S, Itoh S, Grimsby S, Engström U, Heldin C-H, Funa K, Peter ten Dijke. The L45 loop in type I receptors for TGF-β family members is a critical determinant in specifying Smad isoform activation. FEBS Lett. 1998;434:83–7.
36. Ramachandran A, Mehić M, Wasim L, Malinova D, Gori I, Blaszczyk BK, Carvalho DM, Shore EM, Jones C, Hyvönen M, Tolar P. and C. S. Hill. 2021. 'Pathogenic ACVR1(R206H) activation by Activin A-induced receptor clustering and autophosphorylation'. Embo j, 40: e106317.
37. Ramachandran A, Vizán P, Das D, Chakravarty P, Vogt J, Rogers KW, Müller P, Hinck AP, Sapkota GP. and Caroline S. Hill. 2018. 'TGF-β uses a novel mode of receptor activation to phosphorylate

SMAD1/5 and induce epithelial-to-mesenchymal transition', *eLife*, 7: e31756.

38. Ricard N, Bidart M, Mallet C, Lesca G, Giraud S, Prudent R, Feige J-J, Sabine Bailly. Functional analysis of the BMP9 response of ALK1 mutants from HHT2 patients: a diagnostic tool for novel ACVRL1 mutations. Blood. 2010;116:1604–12.
39. Szilágyi SS, Amsalem-Zafran AR, Shapira KE, Ehrlich M, Henis YI. Competition between type I activin and BMP receptors for binding to ACVR2A regulates signaling to distinct Smad pathways. BMC Biol. 2022;20:50.
40. Szilágyi SS, Gutman O, Henis YI. Complex Formation Among TGF-β Receptors in Live Cell Membranes Measured by Patch-FRAP. Methods Mol Biol. 2022;2488:23–34.
41. Townson SA, Martinez-Hackert E, Greppi C, Lowden P, Sako D, Liu J, Ucran JA, Liharska K, Underwood KW, Seehra J, Kumar R, Grinberg AV. Specificity and structure of a high affinity activin receptor-like kinase 1 (ALK1) signaling complex. J Biol Chem. 2012;287:27313–25.
42. Trumpp M, Gatin-Fraudet B, Bruckmann K, Burdzinski W, Roßmann K, Levitz J, Knaus P, Jatzlau J, Broichhagen J. Developing HaloTag and SNAP-Tag Chemical Inducers of Dimerization to Probe Receptor Oligomerization and Downstream Signaling. Angew Chem Int Ed Engl. 2025;64:e202506830.
43. Upton PD, Davies RJ, Trembath RC, Morrell NW. Bone morphogenetic protein (BMP) and activin type II receptors balance BMP9 signals mediated by activin receptor-like kinase-1 in human pulmonary artery endothelial cells. J Biol Chem. 2009;284:15794–804.
44. Valdimarsdottir G, Goumans MJ, Itoh F, Itoh S, Heldin CH, ten Dijke P. Smad7 and protein phosphatase 1alpha are critical determinants in the duration of TGF-beta/ALK1 signaling in endothelial cells. BMC Cell Biol. 2006;7:16.
45. van Caam A, Madej W, Garcia de Vinuesa A, Goumans MJ, Ten Dijke P, Blaney Davidson E, van der P Kraan. TGFβ1-induced SMAD2/3 and SMAD1/5 phosphorylation are both ALK5-kinase-dependent in primary chondrocytes and mediated by TAK1 kinase activity. Arthritis Res Ther. 2017;19:112.
46. Wrana JL, Attisano L, Cárcamo J, Zentella A, Doody J, Laiho M, Wang X-F, Joan Massague. TGFβ signals through a heteromeric protein kinase receptor complex. Cell. 1992;71:1003–14.
47. Wrighton KH, Lin X, Yu PB, Feng XH. Transforming Growth Factor {beta} Can Stimulate Smad1 Phosphorylation Independently of Bone Morphogenic Protein Receptors. J Biol Chem. 2009;284:9755–63.
48. Yadin D, Knaus P, Mueller TD. Structural insights into BMP receptors: Specificity, activation and inhibition. Cytokine Growth Factor Rev. 2016;27:13–34.
49. Zhang H, Du L, Zhong Y, Flanders KC, Roberts JD, Jr. Transforming growth factor-β stimulates Smad1/5 signaling in pulmonary artery smooth muscle cells and fibroblasts of the newborn mouse through ALK1. Am J Physiol Lung Cell Mol Physiol. 2017;313:L615–27.
50. Zhang H, Tian S, Klausen C, Zhu H, Liu R, Leung PC. Differential activation of noncanonical SMAD2/SMAD3 signaling by bone morphogenetic proteins causes disproportionate induction of

hyaluronan production in immortalized human granulosa cells. Mol Cell Endocrinol. 2016;428:17–27.

51. Zhao H-J, Klausen C, Li Y, Zhu H, Wang Y-L, Peter CK, Leung. Bone morphogenetic protein 2 promotes human trophoblast cell invasion by upregulating N-cadherin via non-canonical SMAD2/3 signaling. Cell Death Dis. 2018;9:174.

Figures

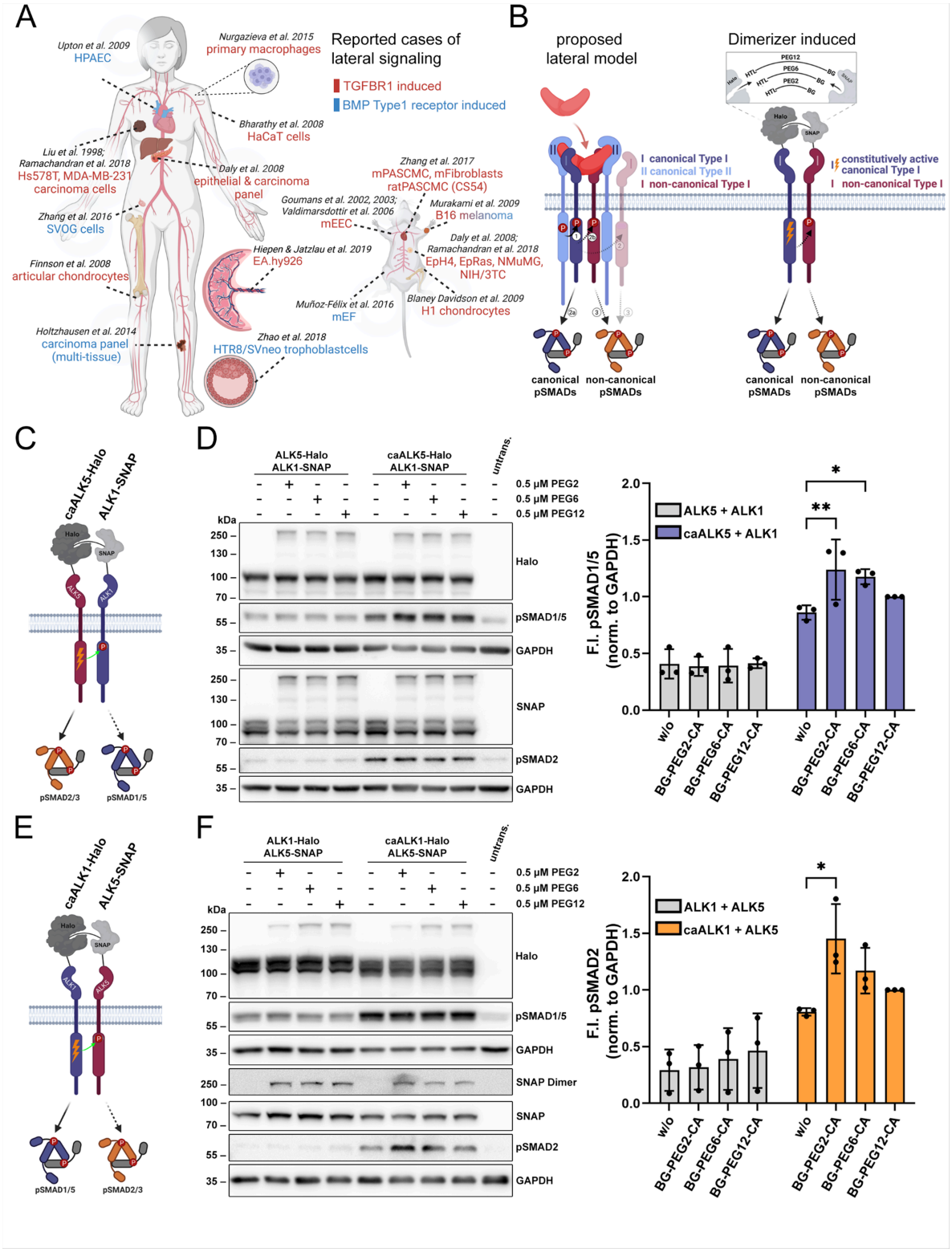


Figure 1

Lateral TGFβ–BMP signaling: forced proximity drives cross-activation of ALK5 and ALK1 in both directions. (**A**) Schematic overview of published evidence for lateral TGFβ and BMP signaling across human and mouse systems; colored by direction: TGFβ-induced (red), BMP-induced (blue). **(B)** Conceptual representation of the proposed lateral model. Within a mixed receptor complex, the type II receptor phosphorylates the canonical type I receptor (1), which then activates its respective R-SMADs

(2a) and cross-activates the non-canonical type I receptor (2b). The non-canonical receptor in turn phosphorylates the opposing R-SMADs (3), so that a single complex yields both canonical (straight arrows) and non-canonical (dashed arrows) pSMADs. This was tested by chemically induced dimerization of Halo- and SNAP-tagged receptors using bifunctional dimerizers of varying linker length. A2/5KO cells were transiently transfected with the indicated Halo- and SNAP-tagged receptor constructs and treated with 0.5 µM dimerizer (BG-PEG_2-HTL, BG-PEG_6-HTL or BG-PEG_{12}-HTL (Trumpp et al. 2025)) for 30 min; GAPDH serves as loading reference. (**C**) Schematic of the forced dimerization of Halo-tagged caALK5 and SNAP-tagged ALK1 and expected downstream SMAD signaling. (**D**) Immunoblot of cells expressing ALK5-Halo or caALK5-Halo with ALK1-SNAP; pSMAD1/5 and pSMAD2 as downstream readout. (right) Densitometric quantification of lateral (non-canonical) pSMAD1/5; *$p < 0.05$, **$p < 0.01$. (**E**) Schematic of the forced dimerization of Halo-tagged caALK1 and SNAP-tagged ALK5 and expected downstream SMAD signaling. (**F**) Immunoblot of cells expressing ALK1-Halo or caALK1-Halo with ALK5-SNAP; pSMAD1/5 and pSMAD2 as downstream readout. (right) Densitometric quantification of lateral (non-canonical) pSMAD2; *$p < 0.05$. Quantifications are normalized to GAPDH and expressed as fold induction relative to the PEG_{12}-treated condition; comparisons were made among the w/o, PEG_2, and PEG_6 conditions of the constitutively active set. Significance was calculated using Tukey's multiple comparisons test against the respective untreated (w/o) condition (n = 3 independent experiments). Schematics created in BioRender (https://BioRender.com/dkvma5w).

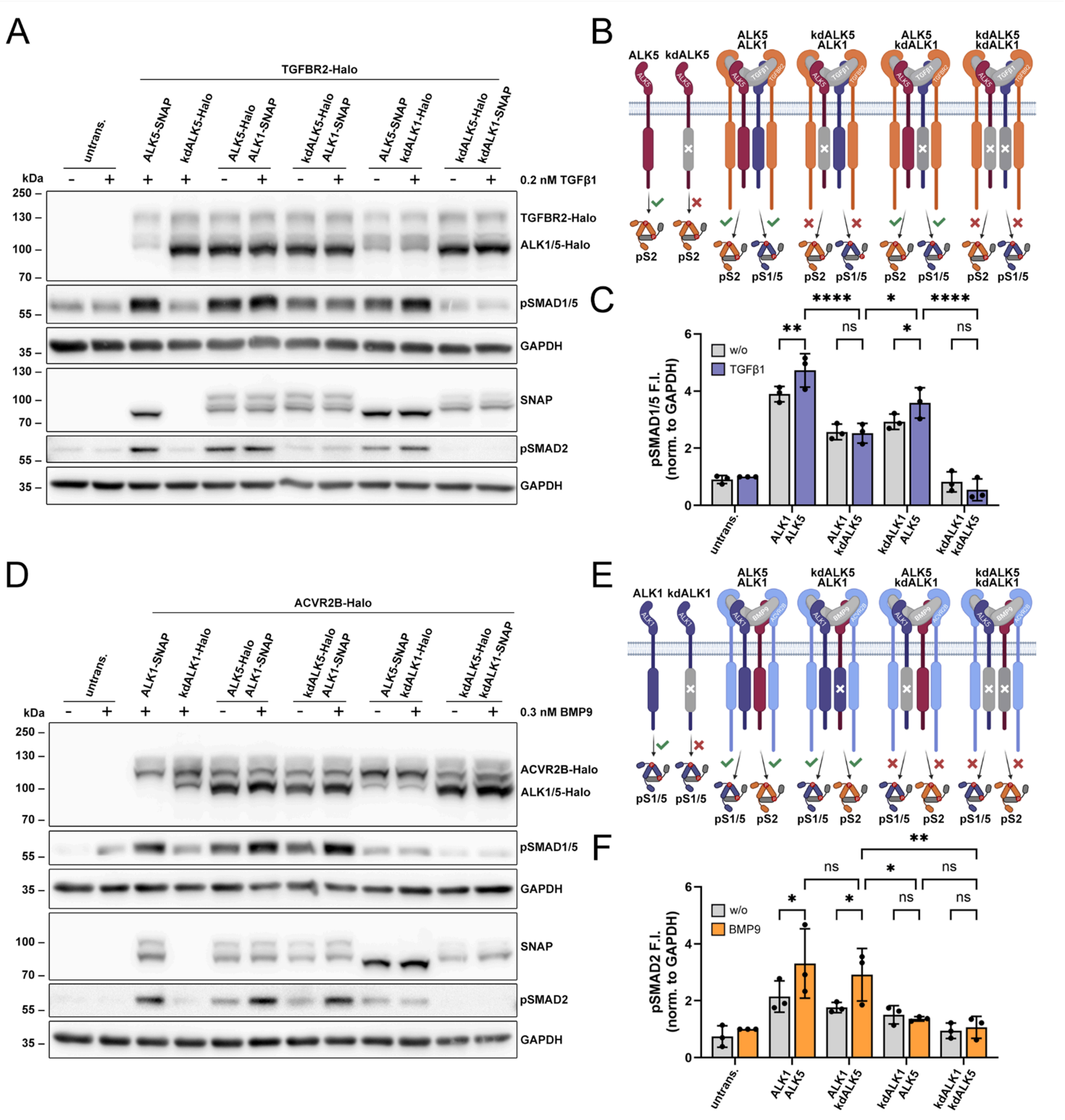


Figure 2

Lateral TGFβ and BMP9 signaling require the kinase activity of their canonical type I receptor. ALK2/5KO cells were transiently transfected with the indicated type II receptor together with Halo- and SNAP-tagged wild-type or kinase-dead ALK1 and ALK5 constructs. In the schematics, silenced kinase domains are shown in gray, and receptors are depicted without their N-terminal Halo- and SNAP-tags for simplicity. pSMAD1/5 and pSMAD2 are abbreviated as pS1/5 and pS2. GAPDH serves as loading

reference throughout. (**A**) Immunoblot of cells co-expressing TGFBR2-Halo and the indicated wild-type or kinase-dead ALK5 and ALK1 constructs, stimulated with 0.2 nM TGFβ1 for 30 min. pSMAD1/5 (lateral) and pSMAD2 (canonical) levels are shown as downstream signaling readouts. (**B**) Schematic of the potential receptor complexes formed by the four wild-type/kinase-dead combinations of ALK5 and ALK1 with TGFBR2, and the observed downstream SMAD signaling for each. (**C**) Densitometric quantification of pSMAD1/5. (**D**) Immunoblot of cells co-expressing ACVR2B-Halo and the indicated wild-type or kinase-dead ALK1 and ALK5 constructs, stimulated with 0.3 nM BMP9 for 60 min. pSMAD1/5 (canonical) and pSMAD2 (lateral) levels are shown as downstream signaling readouts. (**E**) Schematic of the potential receptor complexes formed by the four wild-type/kinase-dead combinations of ALK1 and ALK5 with ACVR2B, and the observed downstream SMAD signaling for each. (**F**) Densitometric quantification of pSMAD2. Quantifications are normalized to GAPDH and expressed as fold induction relative to the untransfected, stimulated condition. Significance was calculated by two-way ANOVA with Tukey's multiple comparisons test, comparing both between the stimulated receptor constructs and between the unstimulated and stimulated condition of each construct; in (**C**) *p < 0.05, **p < 0.01, ****p < 0.0001, and in (**F**) *p < 0.05, **p < 0.01 (ns, not significant) (n = 3 independent experiments). Schematics created in BioRender (https://BioRender.com/dkvma5w).

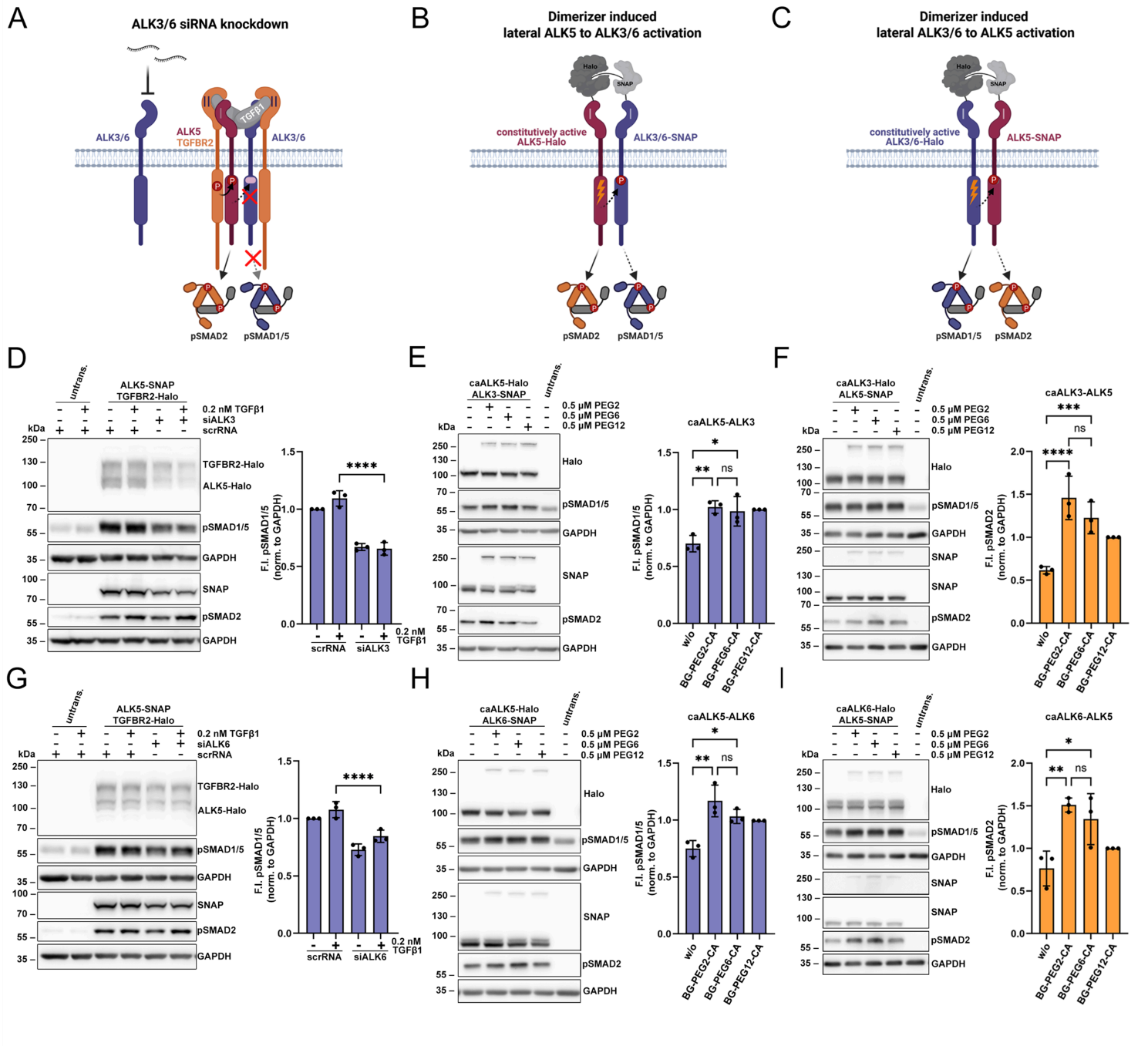


Figure 3

Direct reciprocal lateral activation between ALK5 and the BMP type I receptors ALK3 and ALK6. (**A**) Schematic of the siRNA knockdown approach: endogenous ALK3/6 is depleted to test its contribution to lateral pSMAD1/5 signaling downstream of ALK5. (**B, C**) Schematics of the dimerizer-induced lateral activation approach, showing the two reciprocal pairings: (**B**) caALK5 brought into proximity with ALK3 or ALK6, and (**C**) caALK3 or caALK6 brought into proximity with ALK5. Each panel shows a representative immunoblot with densitometric quantification. For the siRNA panels (**D**, **G**), cells were transfected with ALK5-SNAP and TGFBR2-Halo together with scrambled (scrRNA) or target-specific siRNA and stimulated with 0.2 nM TGFβ1. For the dimerizer panels (**E**, **F**, **H**, **I**), cells expressing the

indicated Halo-/SNAP-tagged constitutively active and wild-type receptor pair were treated with 0.5 μM of the indicated dimerizer for 30 min. (**D**) pSMAD1/5 measured following siALK3 knockdown. (**E**) Lateral pSMAD1/5 induced by proximity of caALK5-ALK3. (**F**) Reciprocal lateral pSMAD2 induced by proximity of caALK3-ALK5. (**G**) pSMAD1/5 measured following siALK6 knockdown. (**H**) Lateral pSMAD1/5 induced by proximity of caALK5-ALK6. (**I**) Reciprocal lateral pSMAD2 induced by proximity of caALK6-ALK5. siRNA experiments were performed in ALK2/5 KO cells and dimerizer experiments were performed in ALK2/4/5 KO cells; GAPDH serves as loading reference throughout. Data are mean ± SD (n = 3 independent experiments) and expressed as fold induction. siRNA panels are normalized to unstimulated scrambled control and analyzed relative to the stimulated scrambled control; dimerizer panels are normalized to the PEG_{12}-treated condition, and statistical comparisons were assessed among the w/o, PEG_2, and PEG_6 conditions. Significance was calculated by two-way ANOVA with Tukey's multiple comparisons test; *p < 0.05, **p < 0.01, ***p < 0.001, ****p < 0.0001 (ns, not significant). Schematics created in BioRender (https://BioRender.com/dkvma5w).

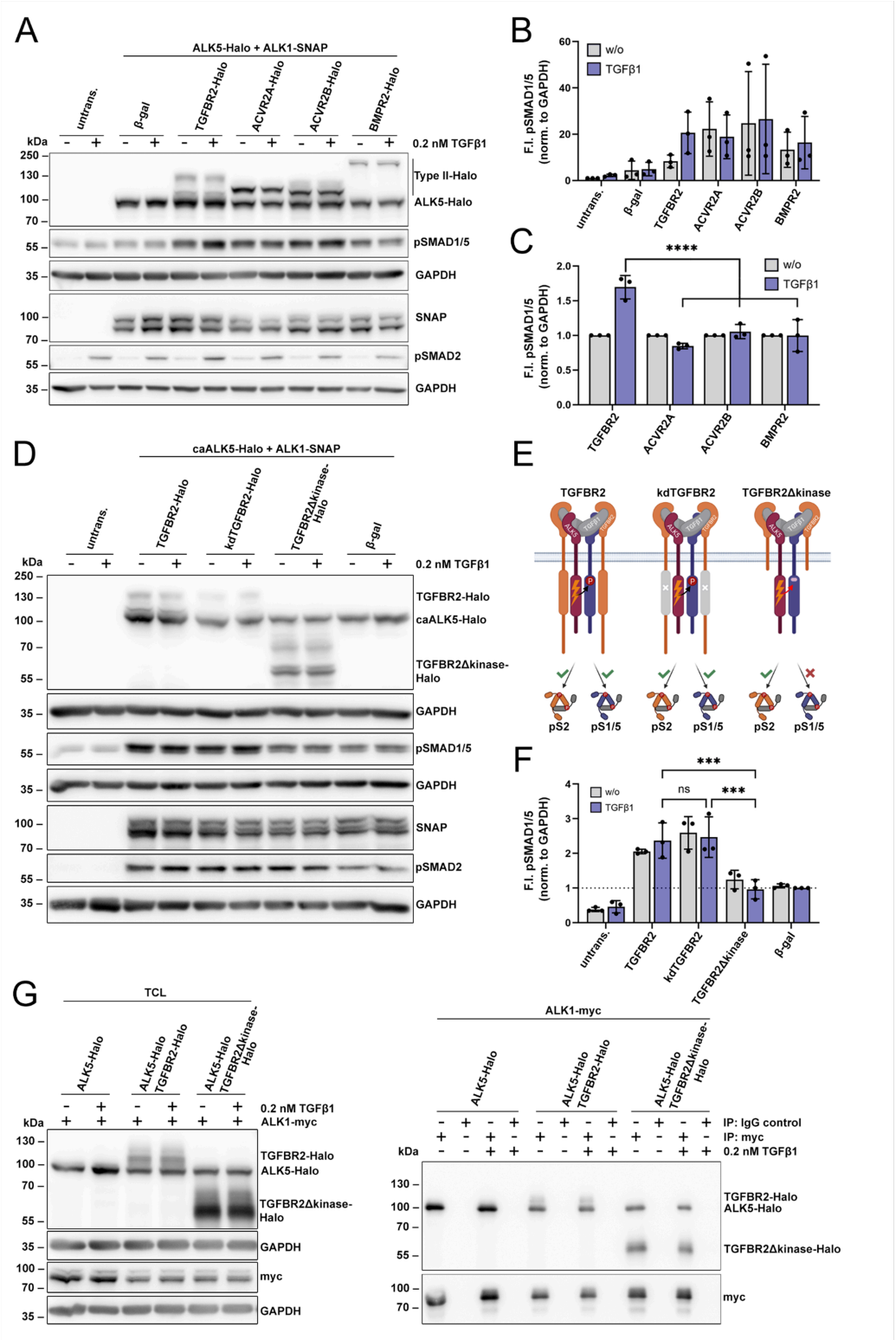


Figure 4

Lateral TGFβ1 signaling requires the kinase domain of TGFBR2 as a scaffold, not its enzymatic kinase activity. (**A**) Immunoblot of ALK2/4 KO cells transiently expressing ALK5-Halo, ALK2-SNAP and one of the Halo-tagged type II receptors TGFBR2, ACVR2A, ACVR2B or BMPR2, starved for 3 h and stimulated with 0.2 nM TGFβ1 for 30 min; pSMAD1/5 (lateral) and pSMAD2 (canonical) as downstream readout. (**B**) Densitometric quantification of lateral pSMAD1/5, normalized to the unstimulated untransfected control

to reflect overall signaling levels. (**C**) Densitometric quantification of lateral pSMAD1/5, with each type II receptor normalized to its respective unstimulated control, reflecting TGFβ1-induced fold change. (**D**) Immunoblot of ALK2/5 KO cells transiently expressing caALK5-Halo, ALK1-SNAP and Halo-tagged TGFBR2, kdTGFBR2 (kinase-dead) or TGFBR2Δkinase (deletion of kinase-domain), starved for 3 h and stimulated with 0.2 nM TGFβ1 for 30 min; pSMAD1/5 (lateral) and pSMAD2 (canonical) as downstream readout. (**E**) Schematic of the ALK1/caALK5/TGFBR2 complexes formed with the three TGFBR2 variants and the observed downstream SMAD signaling. Silenced kinase domains are shown in gray, and receptors are depicted without their respective tags for simplicity. pSMAD1/5 and pSMAD2 are abbreviated as pS1/5 and pS2. (**F**) Densitometric quantification of lateral pSMAD1/5. (**G**) Co-immunoprecipitation of myc-tagged ALK1 from COS-7 cells co-expressing ALK5-Halo either alone or together with TGFBR2-Halo or TGFBR2Δkinase-Halo, with or without stimulation; total cell lysate (left) and myc-tag immunoprecipitate (right). Cells were starved for 24 h and stimulated with 0.2 nM TGFβ1 for 30 min. Blots were probed for Halo-tag and myc-tag; normal mouse IgG serves as immunoprecipitation control. GAPDH serves as loading reference throughout. Quantifications are normalized to GAPDH and expressed as fold induction. In (**C**), comparisons were made among the stimulated type II receptors; in (**F**), values are normalized to the stimulated β-gal control, with comparisons made among the stimulated TGFBR2, kdTGFBR2, and TGFBR2Δkinase conditions. Significance was calculated by two-way ANOVA with Tukey's multiple comparisons test; (**C**) ****$p < 0.0001$, (**F**) ***$p < 0.001$ (ns, not significant) (n = 3 independent experiments). Schematics created in BioRender (https://BioRender.com/dkvma5w).

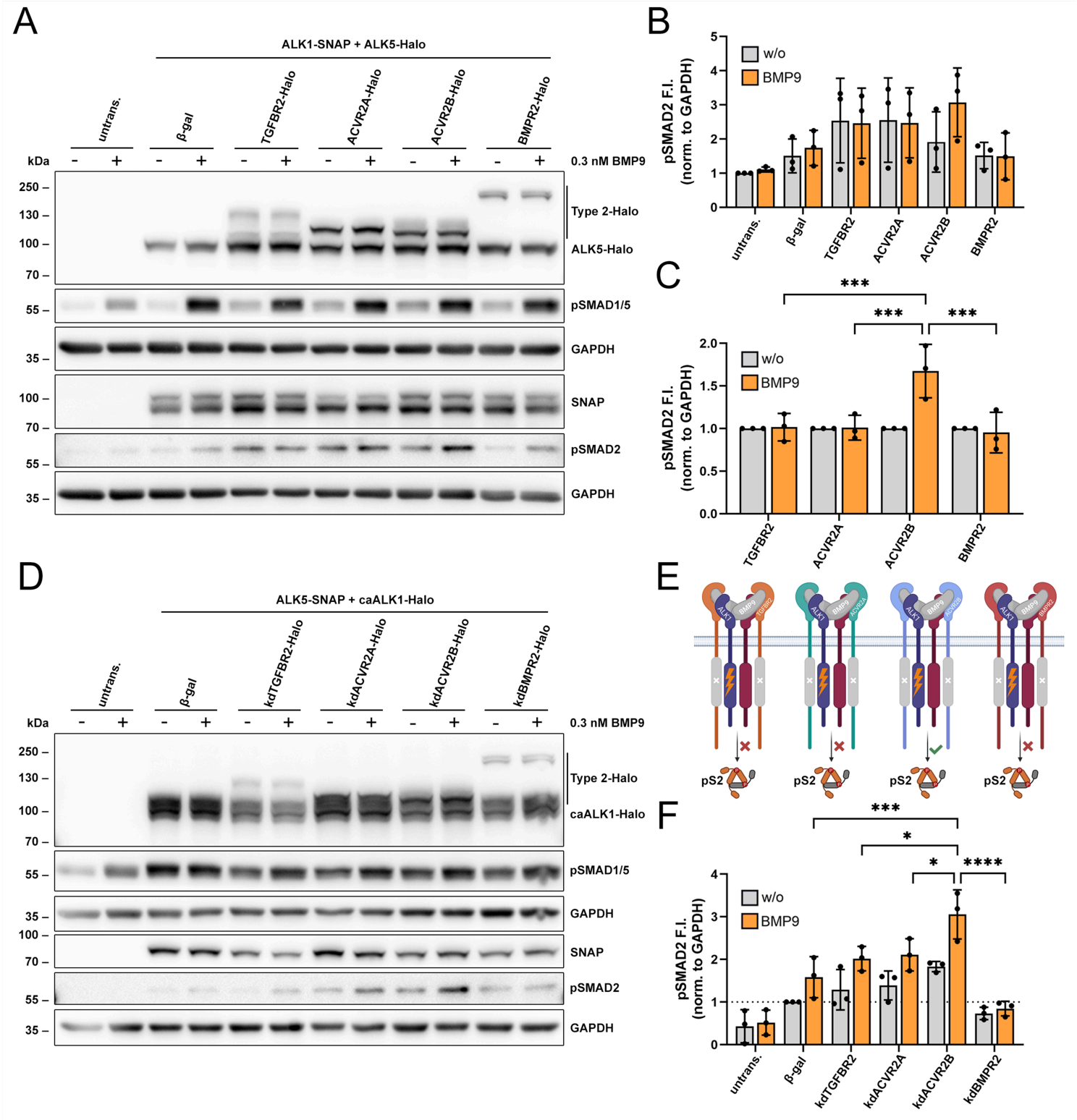


Figure 5

Lateral BMP9 signaling requires the type II receptor ACVR2B. (**A**) Immunoblot of ALK2/4 KO cells transiently expressing ALK5-Halo, ALK1-SNAP and one of the Halo-tagged type II receptors TGFBR2, ACVR2A, ACVR2B or BMPR2, stimulated with 0.3 nM BMP9 for 60 min; pSMAD2 (lateral) and pSMAD1/5 (canonical) as downstream readout. (**B**) Densitometric quantification of lateral pSMAD2, normalized to the unstimulated untransfected control to reflect overall signaling levels. (**C**) Densitometric quantification

of lateral pSMAD2, with each type II receptor normalized to its respective unstimulated control, reflecting BMP9-induced fold change. (**D**) Immunoblot of ALK2/4/5 KO cells transiently expressing caALK1-Halo, ALK5-SNAP and one of the Halo-tagged kinase-dead type II receptors kdTGFBR2, kdACVR2A, kdACVR2B or kdBMPR2, stimulated with 0.3 nM BMP9 for 60 min; pSMAD2 (lateral) and pSMAD1/5 (canonical) as downstream readout. (**E**) Schematic of the caALK1/ALK5 complexes formed with the four kinase-dead type II receptors and the observed downstream SMAD signaling. Silenced kinase domains are shown in gray and receptors are depicted without their respective tags for simplicity. pSMAD1/5 and pSMAD2 are abbreviated as pS1/5 and pS2. (**F**) Densitometric quantification of lateral pSMAD2, normalized to the unstimulated β-gal control. GAPDH serves as loading control. Band intensities were first normalized to GAPDH and then expressed as fold induction relative to the control indicated for each panel. Comparisons were made among the stimulated receptor conditions in (**C**) and (**F**). Significance was calculated by two-way ANOVA with Tukey's multiple comparisons test; (**C**) ***p < 0.001, (**F**) *p < 0.05, ***p < 0.001, ****p < 0.0001 (ns, not significant) (n = 3 independent experiments). Schematics created in BioRender (https://BioRender.com/dkvma5w).

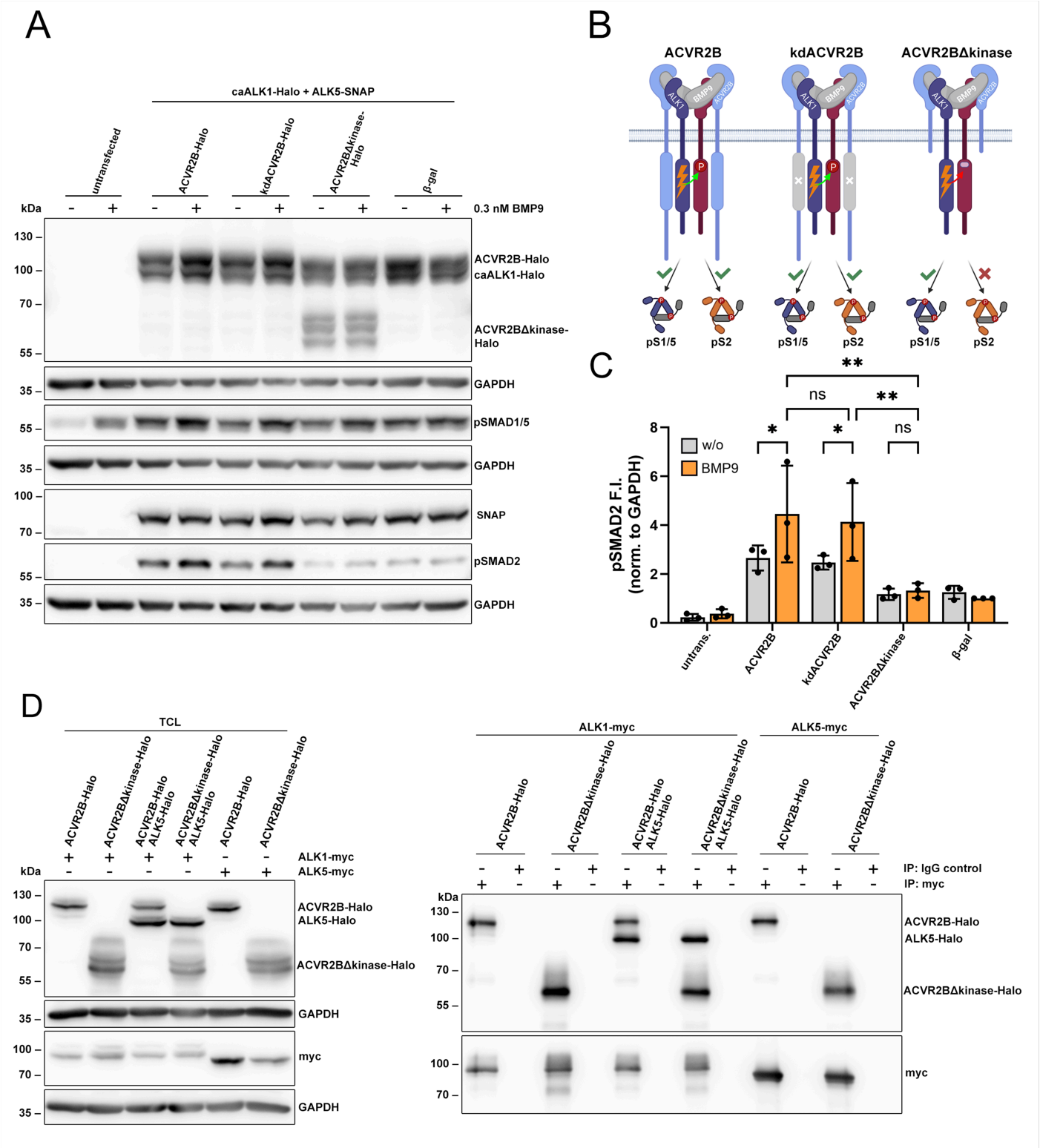


Figure 6

Lateral BMP9 signaling requires the ACVR2B kinase domain as a scaffold. (**A**) Immunoblot of ALK2/4/5 KO cells transiently expressing caALK1-Halo, ALK5-SNAP and Halo-tagged ACVR2B, kdACVR2B (kinase-dead) or ACVR2BΔkinase (kinase-domain deletion), stimulated with 0.3 nM BMP9 for 60 min; pSMAD2 (lateral) and pSMAD1/5 (canonical) as downstream readout. GAPDH serves as loading reference. (**B**) Schematic of the caALK1/ALK5/ACVR2B complexes formed with the three ACVR2B variants and the

observed downstream SMAD signaling; silenced kinase domains are shown in gray, and receptors are depicted without their tags for simplicity. pSMAD1/5 and pSMAD2 are abbreviated as pS1/5 and pS2. (**C**) Densitometric quantification of lateral pSMAD2. (**D**) Co-immunoprecipitation of myc-tagged ALK1 or ALK5 with Halo-tagged ALK5, ACVR2B or ACVR2BΔkinase in COS-7 cells; total cell lysate (left) and myc-tag immunoprecipitate (right). Cells were starved for 24 h and harvested without stimulation. Blots were probed for Halo-tag and myc-tag, with GAPDH as loading reference for the total cell lysate; normal mouse IgG serves as immunoprecipitation control. Quantification in (**C**) is normalized to the stimulated β-gal control and expressed as fold induction. Significance was calculated by two-way ANOVA with Tukey's multiple comparisons test, comparing both between the stimulated receptor constructs and between the unstimulated and stimulated condition of each construct; *$p < 0.05$, **$p < 0.01$ (ns, not significant) (n = 3 independent experiments). Schematics created in BioRender (https://BioRender.com/dkvma5w).

Supplementary Files

This is a list of supplementary files associated with this preprint. Click to download.

- SupplementaryInformation.pdf